Coherence and Coulomb blockade in single-electron devices: A unified treatment of interaction effects

S. Florens,[1] P. San José,[2] F. Guinea,[2] and A. Georges[1]
[1]*Laboratoire de Physique Théorique, Ecole Normale Supérieure, 24 Rue Lhomond, 75231 Paris Cedex 05, France*
[2]*Instituto de Ciencia de Materiales de Madrid, CSIC, Cantoblanco, E-28049 Madrid, Spain*
(Received 14 July 2003; published 15 December 2003)

We study the interplay between Coulomb blockade and the Kondo effect in quantum dots. We use a self-consistent scheme which describes mesoscopic devices in terms of a collective phase variable (slave rotor) and quasiparticle degrees of freedom. In the strong Coulomb blockade regime, we recover the description of metallic islands in terms of a phase-only action. For a dot with well-separated levels, our method leads to the Kondo effect. We identify the regime where a crossover between the Coulomb blockade regime at high temperatures and the formation of a Kondo resonance at lower temperature takes place. In addition, we find that for a dot with many overlapping resonances, an *inverse crossover* can take place. A Kondo resonance which involves many levels within the dot is first formed, and this coherent state is suppressed by correlation effects at lower temperatures. A narrower Kondo resonance, due to a single level in the dot, can emerge at even lower temperatures.

DOI: 10.1103/PhysRevB.68.245311 PACS number(s): 73.23.Hk, 73.63.Kv, 71.10.−w

I. INTRODUCTION

Electron-electron interactions play a crucial role in single electron devices (quantum dots, metallic islands); see, for instance, Refs. 1–4. The electrostatic repulsion between electrons in the dot can be described by the energy required to change the charge in the dot by one unit, E_c. At temperatures or frequencies below this charging energy, but much greater than the spacing between the electronic levels in the dot, δE, Coulomb blockade effects dominate[5–8] and the conductance through the dot is suppressed, except at degeneracy points. At scales below the level splitting within the dot and when the ground state of the dot is degenerate, electronic coherence can be restored by the Kondo effect,[9,10] leading to an increase in the conductance.[11–15] hence, when the charging energy is much greater than the level spacing within the dot, $E_c \gg \delta E$, and the number of electrons in the dot is odd, one expects a crossover between a high-temperature regime where Coulomb blockade effects dominate and a low-temperature one described by the Kondo effect.[16]

The theoretical analysis of these two regimes, Coulomb blockade and the Kondo effect, has been carried out using rather different techniques. Coulomb blockade can be studied when the coupling between the leads and the dot is weak by describing electron transport in terms of sequential hopping processes[2]—i.e., perturbatively in the tunneling matrix element. When the conductance is large, it is convenient to describe the internal degrees of freedom of the dot in terms of a collective variable, the phase conjugated to the total charge.[17–19] Using this representation, the renormalization of the effective charging energy by virtual fluctuations can be studied by a variety of methods.[20–26] This approach becomes exact when the level spacing within the dot tends to zero and the number of transmitting channels is large, which applies in fact to the physical situation of metallic islands. In this limit the Kondo effect disappears. In the opposite limit, when the level spacing within the dot becomes comparable to other scales of interest, the standard procedure is to truncate the Hilbert space of the dot and keep only the interacting electronic states closest to the Fermi level of the leads, so that the system is reduced to the Anderson model;[12,27] see Refs. 11, 28 and 29. The situation when many levels within a magnetic impurity contribute to the Kondo effect was initially discussed in Ref. 30. The same effect in quantum dots was analyzed in Ref. 31. Other modifications of the Kondo effect in a quantum dot due the presence of many levels are discussed in Refs. 32–38. Recent experiments[39] suggest that the regime where level spacing, level broadening, and the charging energy are comparable can be achieved by present day techniques.

The aim of this paper is to analyze the different regimes of a quantum dot characterized by the charging energy E_c, level spacing δE, and coupling to the leads, Γ, where Γ is the typical width of each level. We introduce a new scheme which describes the charge excitations of the dot in terms of a collective phase, but also retains information about the electronic degrees of freedom on the dot. This approach allows us to recover the Kondo effect in the case of quantum impurities with exactly degenerate levels (slave rotor representation introduced in Ref. 40 by two of us). Technically, the new scheme draws inspiration from self-consistent resummations used for describing the Kondo effect in single-impurity models [the so-called noncrossing approximation[41,42] (NCA)] but adapted in an economical way to the situation of mesoscopic structures (which can contain up to thousands of electrons).

The outline of this paper is as follows. In Sec. II we review basic properties of the single-electron box and present the model that we will study throughout. The self-consistent approach used to analyze the model is presented in Sec. III and will be shown to describe the Coulomb blockade regime of metallic grains *exactly* (also for quantum dots); we will furthermore show that it is a reasonable approximation for dealing with the Kondo effect (in quantum dots). In Sec. IV we will investigate in more detail intermediate regimes of

conduction that were not previously attainable or considered in earlier works. In particular we will be interested in the different manner in which one goes from coherent, Kondo-assisted transport to the Coulomb blockade regime. Extensions of our approach to other systems such as quantum dot arrays will be briefly outlined in the Conclusion.

II. MODEL FOR SINGLE-ELECTRON DEVICES

A. Phase representation and electronic degrees of freedom

Let us first review the standard model for single-electron devices. The basic ingredient that determines the behavior of quantum dots as well as metallic islands is the relatively large Coulomb energy $E_c=e^2/(2C)\sim 1$ K associated with small capacitances of the structure, $C\sim 10^{-15}$ F. We will take also into account the internal structure of the small charge droplet, with energy levels ϵ_p (which are shape and disorder dependent) and an index $\sigma=1,\ldots,\mathcal{N}$ associated with transmitting channels to the outside circuit. The electrodes, to which the mesoscopic region is coupled, are described as Fermi liquids with a spectrum ε_k associated with a finite density of states $D(0)$ at the Fermi level. Physical quantities, such as the conductance G, are also determined as a function of temperature T (we set $\beta\equiv 1/T$) and applied gate voltage V_g. Summarizing all these energy scales, we arrive at the following Hamiltonian:

$$H=\sum_{k\sigma}\varepsilon_k a^\dagger_{k\sigma}a_{k\sigma}+\sum_{p\sigma}\epsilon_p d^\dagger_{p\sigma}d_{p\sigma} +E_c\left(\sum_{p\sigma} d^\dagger_{p\sigma}d_{p\sigma}-n_g\right)^2+\sum_{k\sigma p}t^p_k(a^\dagger_{k\sigma}d_{p\sigma}+d^\dagger_{p\sigma}a_{k\sigma}). \tag{1}$$

We have introduced here the coupling t^p_k between the mode p in the electrode and mode k in the electron box. The index $p=1,\ldots,N_L$ corresponds to the N_L energy levels of the dot (or metallic island), and $\sigma=1,\ldots,\mathcal{N}$ is the conserved channel index (including spin). We defined also n_g as a dimensionless external gate voltage, $n_g\equiv eV_g/(2E_c)$. Because of the large number of degrees of freedom involved with respect to a single-impurity Anderson model (N_L or $\mathcal{N}$ can be quite large), this Hamiltonian is remarkably complicated.

One way to make progress is to single out the relevant charge variable on the dot and pilot its dynamics by means of a rotor degree of freedom:

$$\sum_{p\sigma} d^\dagger_{p\sigma}d_{p\sigma}=\hat{L}=-i\partial/\partial\theta. \tag{2}$$

This mapping is motivated by the fact that the Hamiltonian $H_{\rm rotor}=E_c\hat{L}^2$, with its quadratic spectrum, reproduces exactly the charging energy term in Eq. (1). Alternatively, one can argue, as in Refs. 17 and 18, that a metallic grain can be studied with the same formalism used for a superconducting grain, except that the gap vanishes. In this case, the phase is the collective variable conjugate to the number of particles, as implied by Eq. (2).

In order to fulfill the Pauli principle, one must, however, keep fermionic degrees of freedom, so that the creation of a physical electron on the dot is represented as

$$d^\dagger_{p\sigma}=f^\dagger_{p\sigma}e^{i\theta} \tag{3}$$

using a channel- and momentum-carrying quasiparticle $f^\dagger_{p\sigma}$. According to Eq. (2), a constraint $\hat{L}=\Sigma_{p\sigma}f^\dagger_{p\sigma}f_{p\sigma}$ must also be implemented,[40] introducing for this purpose a Lagrange multiplier $\delta\mu$. Integrating explicitly the electrode in Eq. (1), one gets the following expression for the action of the original model in this new representation:

$$S=\int_0^\beta d\tau\sum_{p\sigma} f^\dagger_{p\sigma}(\partial_\tau+\epsilon_p-\delta\mu)f_{p\sigma} +\frac{(\partial_\tau\theta+i\delta\mu)^2}{4E_c}+in_g\partial_\tau\theta +\int_0^\beta d\tau\int_0^\beta d\tau'\frac{1}{N_L}\sum_{pp'\sigma}\Delta^{pp'}(\tau-\tau') \times f^\dagger_{p\sigma}(\tau)f_{p'\sigma}(\tau')e^{i\theta(\tau)-i\theta(\tau')}. \tag{4}$$

In principle, $\delta\mu$ should be integrated over $[0,2\pi/\beta]$ in order to preserve the correct structure of the Hilbert space. One can notice in this expression how the indices are positioned in the last term (σ is conserved by the charge transfer procedure, whereas p is not). We also have defined the bath function

$$\Delta^{pp'}(i\omega)\equiv\sum_k\frac{N_L t^p_k t^{p'}_k}{i\omega-\varepsilon_k}=\int d\varepsilon D(\varepsilon)\frac{N_L t^p(\varepsilon)t^{p'}(\varepsilon)}{i\omega-\varepsilon}, \tag{5}$$

introducing the lead density of states $D(\varepsilon)=\Sigma_k\delta(\varepsilon-\varepsilon_k)$ (we have extracted here a factor $1/N_L$ for future convenience).

B. Metallic grains: Phase-only approach

In the case of small metallic islands,[6,7] the number of transverse channels, $\mathcal{N}\sim 10^4$–$10^6\gg 1$, is quite large, so that the fermionic degrees of freedom can be integrated out explicitly from Eq. (4). Technically, this is done by expanding the initial action (4) in the coupling function $\Delta^{pp'}(\tau)$, leading to an exact expression of the effective action:

$$S[\theta]=\int_0^\beta d\tau\frac{(\partial_\tau\theta+i\delta\mu)^2}{4E_c}+in_g\partial_\tau\theta-\ln\sum_{n=0}^\infty\frac{(-1)^n}{n!} \times\left\langle\prod_{m=1}^n\int_0^\beta d\tau_m\int_0^\beta d\tau'_m\frac{1}{N_L}\sum_{p_m p'_m\sigma_m}\Delta^{p_m p'_m}(\tau_m-\tau'_m) \times e^{i\theta(\tau_m)-i\theta(\tau'_m)}f^\dagger_{p_m\sigma_m}(\tau_m)f_{p'_m\sigma_m}(\tau'_m)\right\rangle_0. \tag{6}$$

The average over the fermionic variables $\langle\cdots\rangle_0$ in the preceding expression is taken with respect to the free fermionic

action $S_0=\int_0^\beta d\tau \Sigma_{p\sigma} f_{p\sigma}^\dagger(\partial_\tau+\epsilon_p-\delta\mu)f_{p\sigma}$ and simplifies considerably in the large-$\mathcal{N}$ limit because Wick contractions at leading order occur between pairs of fermions holding the *same* channel index σ_m. We can then reexponentiate the last term in Eq. (6), and if one notes that the multiplier $\delta\mu$ can be treated in the grand canonical ensemble—i.e., reabsorbed in n_g (due to small charge fluctuations over many accessible states)—one gets the effective phase-only action

$$S[\theta]=\int_0^\beta d\tau \frac{(\partial_\tau\theta)^2}{4E_c}+in_g\partial_\tau\theta - \int_0^\beta d\tau\int_0^\beta d\tau'\,\alpha_0(\tau-\tau')e^{i\theta(\tau)-i\theta(\tau')}. \quad (7)$$

The kernel $\alpha_0(\tau)$ in the last equation is given by the expression

$$\alpha_0(\tau)=-\frac{1}{N_L}\sum_{pp'\sigma}\Delta^{pp'}(\tau)\langle f_{p\sigma}^\dagger(\tau)f_{p'\sigma}(0)\rangle_0, \quad (8)$$

which can be evaluated:

$$\alpha_0(\tau)\simeq\alpha_t\frac{(\pi/\beta)^2}{[\sin(\pi\tau/\beta)]^2}, \quad (9)$$

with

$$\alpha_t=\mathcal{N}N_L t^2 D(0)\rho_0(0). \quad (10)$$

Here $\rho_0(\epsilon)=\Sigma_p\delta(\epsilon-\epsilon_p)$ is the grain density of states, which is supposed to be continuous for metallic islands, and we have taken the large bandwidth limit to obtain Eq. (9). We have also assumed for simplicity that the coupling to the lead is a constant, $t_k^p=t$ (point contact) and that it is sufficiently small so that α_t is at most of order 1 when both N_L and $\mathcal{N}$ are large. The parameter α_t is interpreted as the (dimensionless) high-temperature conductance between the dot and island, to lowest order in the hopping t.[17,18,22]

Physically, the use of the phase-only action[22] is vindicated by the fact that the charge fluctuations are suppressed by the Coulomb blockade phenomenon, allowing one to forget about the fermionic statistics of the charge carriers (incoherent transport through the island).

This phase-only action (7) can be handled using a variety of techniques.[20–26] An important question, which is very relevant for experiments on small metallic grains strongly coupled to the environment,[8,43] is the destruction of Coulomb blockade in the strong-tunneling regime $\alpha_t\gtrsim 0.1$. This implies a generic renormalization of the Coulomb energy E_c towards smaller values, denoted here by E_c^*.[21,23] In the following, we will be more interested in this question in the context of quantum dots, for which the model (7) is inadequate. However, the phase-only approach will be considered as an important benchmark for any approach that intends to describe the Coulomb blockade regime.

III. UNIFIED APPROACH TO SINGLE-ELECTRON DEVICES

A. Self-consistent scheme

Our purpose here is to develop a simple approximation scheme [avoiding direct numerical solution of model (1)] that could encompass the main interaction effects in single-electron devices: the Coulomb blockade and Kondo effects. One can note that one is usually forced to employ different techniques to handle the Coulomb interaction, depending on the regime one is interested in. Since the details of the dynamics of the electrons are not usually involved in the Coulomb blockade phenomenon, introducing the total charge as the physically relevant variable and using the phase-only action (7) seems mandatory to deal with this regime. On the other hand, dealing with the Kondo effect requires a rather sophisticated treatment of the correlation effects among electrons, and a simplification of the initial model (1) is unavoidable. We will see in this paper that one can reconcile these two paradigms if one treats on an equal footing fermionic degrees of freedom and the phase variable conjugated to the total charge.

Drawing inspiration from strong coupling approaches for single-impurity models [NCA (Ref. 41) and its generalization to the phase representation (2) as introduced by two of us[40]], we will perform a self-consistent decoupling of the fermion-rotor coupling in Eq. (4):

$$S\simeq\int_0^\beta d\tau\sum_{p\sigma} f_{p\sigma}^\dagger(\partial_\tau+\epsilon_p-\delta\mu)f_{p\sigma} + \int_0^\beta d\tau\int_0^\beta d\tau'\frac{1}{N_L}\sum_{pp'\sigma}\Delta^{pp'}(\tau-\tau') \times\langle e^{i\theta(\tau)-i\theta(\tau')}\rangle f_{p\sigma}^\dagger(\tau)f_{p'\sigma}(\tau') \quad (11)$$

$$+\int_0^\beta d\tau\frac{(\partial_\tau\theta+i\delta\mu)^2}{4E_c}+in_g\partial_\tau\theta + \int_0^\beta d\tau\int_0^\beta d\tau'\frac{1}{N_L}\sum_{pp'\sigma}\Delta^{pp'}(\tau-\tau') \times\langle f_{p\sigma}^\dagger(\tau)f_{p'\sigma}(\tau')\rangle e^{i\theta(\tau)-i\theta(\tau')}. \quad (12)$$

This approximation goes far beyond the lowest-order perturbative result that led to the phase-only action (7) and is the central starting point of the present work. Its distinctive feature is the decoupling of fermionic and phase degrees of freedom, whose joint dynamics is nevertheless determined *self-consistently*. Indeed, the fermionic self-energy obviously depends on the phase-phase correlator and reciprocally. Moreover, the bosonic part of the effective action (12) is similar in structure to the phase-only approach (7), allowing to use the large body of work on this particular model.

In order to detail the method of solution, we start here by simplifying the kernels appearing in the previous self-consistent action. The bosonic kernel can be expressed in terms of the full propagator $G_f^{pp'}$ of the $f_{p\sigma}^\dagger$ fermions:

$$\alpha(\tau) \equiv -\frac{1}{N_L}\sum_{pp'\sigma}\Delta^{pp'}(\tau)\langle f^{\dagger}_{p\sigma}(\tau) f_{p'\sigma}(0)\rangle$$

$$= -\mathcal{N}\frac{1}{N_L}\sum_{pp'}\Delta^{pp'}(\tau) G_f^{pp'}(-\tau), \tag{13}$$

where the Green's function $\hat{G}_f$ has been introduced in a matrix notation,

$$\hat{G}_f = \left[\hat{G}_0^{-1} - \frac{1}{N_L}\hat{\Sigma}_f\right]^{-1} = \hat{G}_0\left[1 - \frac{1}{N_L}\hat{\Sigma}_f\hat{G}_0\right]^{-1}, \tag{14}$$

with the free propagator in the electron box:

$$G_0^{pp'}(i\omega) = \frac{\delta_{pp'}}{i\omega - \epsilon_p + \delta\mu}. \tag{15}$$

We also have introduced the self-energy of the quasiparticles:

$$\Sigma_f^{pp'}(\tau) = \Delta^{pp'}(\tau)\langle e^{i\theta(\tau) - i\theta(0)}\rangle. \tag{16}$$

The ''self-consistent phase action'' that one needs to solve finally reads

$$S = \int_0^\beta d\tau \frac{(\partial_\tau\theta + i\,\delta\mu)^2}{4E_c} + i n_g \partial_\tau\theta$$

$$- \int_0^\beta d\tau \int_0^\beta d\tau'\,\alpha(\tau - \tau') e^{i\theta(\tau) - i\theta(\tau')}, \tag{17}$$

with $\alpha(\tau)$ given previously. The set of equations (13)–(17) is the main technical result of this paper. In practice, this is solved by an iterative procedure which starts with a given kernel $\alpha(\tau)$ as input to the action (17), from which a new correlator $\langle e^{i\theta(\tau) - i\theta(\tau')}\rangle$ is computed. It is then fed back to the self-energy (16), allowing us to compute the quasiparticle propagator (14), and then a new kernel $\alpha(\tau)$ from Eq. (13). This full cycle is repeated until convergence is reached.

In all further calculations, we will assume a point contact between lead and box, $t_k^p = t$, so that $\Delta^{pp'}(\tau) = \Delta(\tau)$ and $\Sigma_f^{pp'}(\tau) = \Sigma_f(\tau) = \Delta(\tau)\langle e^{i\theta(\tau) - i\theta(\tau')}\rangle$, which allows us to simplify expressions (13) and (14) into

$$\alpha(\tau) = -\mathcal{N}\Delta(\tau) G_f^{loc}(-\tau), \tag{18}$$

$$G_f^{loc}(i\omega) \equiv \frac{1}{N_L}\sum_{pp'} G_f^{pp'}(i\omega), \tag{19}$$

$$[G_f^{loc}(i\omega)]^{-1} = \frac{1}{\frac{1}{N_L}\sum_p \frac{1}{i\omega - \epsilon_p + \delta\mu}} - \Sigma_f(i\omega). \tag{20}$$

In the following two paragraphs, we will sketch how this novel scheme allows us to capture both Coulomb blockade and Kondo effects in single-electron devices.

B. Metallic islands: Coulomb blockade

We consider here the case of a metallic island for which the energy spectrum is taken as a continuous density of states $\rho_0(\epsilon)$. Due to the smallness of the Fermi wavelength with respect to the typical transverse size of the island, the number of transmitting channels is usually quite large, $\mathcal{N} \gg 1$, as discussed before in Sec. II B.

One interesting remark is that our self-consistent phase model (11) and (12) *exactly* reproduces the phase-only approach (7) in this case. Indeed, we note that the fermionic self-energy (16) is suppressed with respect to the kernel (18) by a relative factor of order $1/\mathcal{N}$. The self-consistency between fermions and the phase variable can therefore be ignored at $\mathcal{N} \gg 1$ (one has to scale $t \propto 1/\sqrt{\mathcal{N}}$), leading to a free fermionic propagator

$$G_0^{pp'}(\tau) \equiv \langle f^{\dagger}_{p\sigma}(0) f_{p'\sigma}(\tau)\rangle_0, \tag{21}$$

$$G_0^{pp'}(i\omega) = \frac{\delta_{pp'}}{i\omega - \epsilon_p}. \tag{22}$$

Putting this expression back into Eq. (13), one recovers indeed the phase-only action (7) and (8). This test case implies that our self-consistent scheme allows us to deal correctly with the Coulomb blockade phenomenon in metallic grains.

C. Quantum dots: Interaction effects

In quantum dots, the discreteness of the energy spectrum ϵ_p and the fact that $\mathcal{N}$ is generally of order 1 (unless the point contacts are quite open) invalidate the phase-only approach (7). This is clear from the fact that coherent transport through the dot can be restored due to the Kondo effect at low temperature. We now sketch how the self-consistent action (17) is able to describe this phenomenon.

1. Coulomb blockade regime in quantum dots

We consider first temperatures smaller than the charging energy E_c, but still greater than the interlevel spacing δE. We can therefore take a continuous limit for the dot (due to thermal smearing of the energy levels), which leads crudely to the simplification

$$\frac{1}{N_L}\sum_p \frac{1}{(i\omega - \epsilon_p + \delta\mu)} \simeq -i\pi\rho_0(0). \tag{23}$$

From Eq. (20), this gives the $f^{\dagger}_{p\sigma}$ fermion propagator in the dot:

$$G_f^{loc}(i\omega) \simeq \left[\frac{i}{\pi\rho_0(0)} - \Sigma_f(i\omega)\right]^{-1}. \tag{24}$$

The constant imaginary part in the last expression dominates the long-time behavior of the Green's function $G_f^{loc}(\tau)$, so that the kernel (18) decays as $1/\tau^2$, similarly to the case of the metallic island, Eq. (9). There is therefore Coulomb blockade in this regime, as expected.

2. Kondo effect in quantum dots: First discussion

At temperatures below the interlevel spacing δE in the dot, the discreteness of the spectrum becomes sizable. Let us assume here that a single level sits close to the Fermi energy, so that we can forget all other levels. In this case, we can argue here that the factorization (11) and (12) reproduces the Kondo physics correctly. This property is well known if, instead of the phase variable θ, one uses a slave-boson representation of the interaction (in the case of the $E_c=\infty$ limit).[44] This method has been extended recently by two of us to the case of finite E_c, using the phase representation $d^\dagger_{p\sigma}=f^\dagger_{p\sigma}e^{i\theta}$,[40] and shown to lead to a good approximation scheme for dealing with the Kondo effect.

In quantum dots, the Kondo effect manifests itself by the buildup of a many-body resonance close to the Fermi level that allows coherent transport of charge through the structure. The existence of the Friedel sum rule (to be discussed later on) guarantees that the conductance through the dot can recover the unitarity limit (i.e., $G=2e^2/h$) at low temperature.

In conclusion, we can therefore expect that our self-consistent approach interpolates between the coherent Kondo regime (associated with a large and increasing conductance with decreasing temperature) and the Coulomb blockade (which leads to a suppression of the charge fluctuations on the dot and a decreasing conductance). In practice, we still need to solve the self-consistent phase problem (11) and (12). This will be done in the next section.

IV. INTERMEDIATE CONDUCTION REGIMES IN QUANTUM DOTS

A. Solution of the phase action in the spherical limit

The simplest, yet nontrivial treatment of the bosonic action (17) is to take its spherical limit[40,45,46] (this is also equivalent to the large number of component limit for the σ model in the field theory literature[47]). We introduce for this purpose the complex phase field $X(\tau)\equiv e^{i\theta(\tau)}$, with its correlator $G_X(\tau)\equiv\langle X(\tau)X^*(0)\rangle$. This representation is perfectly equivalent to the original problem if the hard constraint $|X(\tau)|^2=1$ is maintained exactly. The approximation that we will make in order to solve the (self-consistent) phase action (17) is to impose this constraint on average only. For this we introduce a Lagrange multiplier λ to enforce the equality $G_X(\tau=0)=\langle|X(\tau)|^2\rangle=1$. The main drawback (on a qualitative level) of this approximation is that, although it works fine close to the center of the charge plateaus, it eventually breaks down at the degeneracy points.[40] We will also enforce the constraint $\Sigma_{p\sigma}f^\dagger_{p\sigma}f_{p\sigma}=\hat{L}$ on average. In the symmetric case (i.e., at the center of a plateau), this simply implies that $\delta\mu=0$.

The bosonic action is now purely quadratic, leading to the set of self-consistent equations[57]

$$G_X(i\nu_n)=\left[\frac{\nu_n^2}{2E_c}+\lambda-\alpha(i\nu_n)\right]^{-1}, \tag{25}$$

$$G_X(\tau=0)=1, \tag{26}$$

$$G_f^{loc}(i\omega_n)=\left[\frac{1}{\frac{1}{N_L}\sum_p 1/(i\omega_n-\epsilon_p)}-\Sigma_f(i\omega_n)\right]^{-1}, \tag{27}$$

$$\alpha(\tau)=\mathcal{N}\Delta(\tau)G_f^{loc}(\tau), \tag{28}$$

$$\Sigma_f(\tau)=\Delta(\tau)G_X(\tau), \tag{29}$$

with the notation

$$\Delta(i\omega_n)=\sum_k \frac{N_L t^2}{i\omega_n-\varepsilon_k}. \tag{30}$$

We have noted here ω_n (ν_n) a fermionic (bosonic) Matsubara frequency. In addition to the relative simplicity of this scheme, we note that it allows us to obtain a solution for real frequency quantities (doing the analytic continuation of these equations), as required for computing spectral and transport properties of quantum dots.

A few technical remarks. The system of equations (25)–(30) was derived previously for the single-level Anderson model[40] using a slightly different route (namely, a large-M multichannel point of view more suitable to understand some non-Fermi-liquid aspects of the solution). We feel that a two-step procedure that starts with Eqs. (11) and (12) is more appealing in the present context, as the self-consistent phase action (12) can be tackled in principle with variety of methods. We have therefore taken the point of view of simplicity in doing the spherical limit described in the previous paragraph.

The numerical solution of the coupled integral equations is straightforward using fast Fourier transforms (we will also give analytical arguments later on). In all calculations that follow, we take $\mathcal{N}=2$ (single channel of conduction per spin). The Coulomb energy is chosen as the reference, $E_c=1$, and the bandwidth of the continuous density of states of the electrodes is $\Lambda=50$, which is the largest energy scale of the problem. The precise form of the spectrum in the electrodes playing little role in the low-energy limit, we have chosen a semielliptic density of states:

$$\Delta(i\omega)=N_L|t|^2\frac{8}{\Lambda^2}[i\omega-i\,\mathrm{sgn}(\omega)\sqrt{\omega^2+(\Lambda/2)^2}]. \tag{31}$$

The *single-level* width $\Gamma\equiv|\mathrm{Im}\,\Delta(i0^+)|/N_L=4t^2/\Lambda$ [see Eq. (4)] characterizes the strength of the coupling of the electrons in the dot to the reservoirs. Other important parameters, which we will also investigate, are the separation between the electronic levels of the dot, δE, and the number of states in the dot, N_L. We also define a typical "bandwidth" of the dot, $W=\delta E(N_L-1)$ (although the spectrum is made up of discrete states).

A technical aspect worth mentioning is the method of computation of the conductance through the dot. In the same spirit of the decoupling performed in Eqs. (11) and (12), we will compute the Green's function of the *physical* electron as $G_d^{loc}(\tau)=G_f^{loc}(\tau)G_X(\tau)$. An analytical continuation (performed numerically) allows us then to get the (interacting)

density of states in the dot, $\rho_d(\omega) = -(1/\pi)\mathrm{Im}\, G_d^{loc}(\omega + i0^+)$. We will also use the interacting Landauer formula for the conductance[28]:

$$G = \frac{\mathcal{N}e^2}{h} N_L \Gamma \int \mathrm{d}\omega \left(-\frac{\partial n_F(\omega)}{\partial \omega} \right) \pi \rho_d(\omega), \qquad (32)$$

where $n_F(\omega) = 1/(e^{\beta\omega}+1)$ is the Fermi function. This expression involves the ''local'' density of states (i.e., summed over all $p = 1, \ldots, N_L$) because of the form of the local coupling to the reservoir, see Eq. (1).

In the following, we explore situations that are intermediate to the single-level Kondo effect and the Coulomb blockade regime, depending on the internal structure of the quantum dot. We insist on the fact that the results that we will obtain are not easily accessible to usual approaches of the Hamiltonian (1), unless only a few levels in the dot are considered (for which case the numerical renormalization group is quite successful[37,48]).

B. Results for finite interlevel spacing: Kondo effect and Coulomb blockade

We now analyze the case of a few, well separated energy levels in the dot. We start by discussing the Coulomb blockade using the spherical limit (for temperature larger than the interlevel spacing); then we give analytical arguments in favor of the existence of a Kondo resonance at lower temperature, and finally we show the full numerical solution of the self-consistent equations corresponding to the usual situation found in experiments.

1. Renormalized Coulomb energy

As discussed in Sec. III C 1, for $T \gg \delta E$ the quantum dot is in the Coulomb blockade regime, and the bosonic kernel (28) behaves at long times as $\alpha(\tau) \sim \alpha_t/\tau^2$; see Eq. (9). Here α_t is a measure of the dimensionless high-temperature conductance. One can now focus on Eq. (26), which we write (at low temperature) as

$$\int \frac{\mathrm{d}\nu}{2\pi} \frac{1}{\nu^2/(2E_c) + \pi\alpha_t|\nu| + \lambda - \alpha(i0)} = 1. \qquad (33)$$

The renormalized Coulomb energy E_c^* is obtained as the mass term in the phase propagator (25), which decays exponentially over time scales of order $\hbar/E_c^*$. Solving the previous equation, one gets

$$E_c^* = \frac{\lambda - \alpha(i0)}{\pi\alpha_t} = 2\pi\alpha_t E_c e^{-\pi^2\alpha_t}, \qquad (34)$$

which is exponentially small in the bare conductance α_t. This quick calculation allows us to understand the origin of the Coulomb blockade for quantum dots in our formalism.

2. Single-level Kondo effect: Analytical proof

In quantum dots, the basic manifestations of the Kondo effect are twofold: the existence of a small energy scale, the Kondo temperature T_K, and restoration of the unitarity limit (at $T < T_K$), as discussed in Sec. III C 2.

To prove the first point from our integral equations (25)–(30), we examine qualitatively the solution of the self-consistent equations at temperatures smaller than the interlevel spacing δE. There, the fermionic Green's function (27) is dominated by the $\epsilon_p = 0$ pole, so that $G_f^{loc}(\tau) \sim -1/(2N_L)\mathrm{sgn}(\tau)$, at long times. From Eq. (28), this produces in turn a rotor self-energy $\alpha(i\nu) \sim -(2\mathcal{N}\Gamma/\pi)\ln|\nu/T_0|$ at low frequency (here T_0 is an undetermined cutoff, in practice of order $\sqrt{E_c\Gamma}$). Upon lowering the temperature, this self-energy can reach the charging energy E_c (assumed to be only weakly renormalized), indicating the suppression of Coulomb blockade and the beginning of the Kondo regime. This happens (very roughly) for $-(2\mathcal{N}\Gamma/\pi)\log(T_K/T_0) \sim E_c$, giving the estimate

$$T_K(N_L) = T_0 \exp\left(-\frac{\pi E_c}{2\mathcal{N}\Gamma} \right) = T_0 \exp\left(-\frac{\pi U}{8\Gamma} \right). \qquad (35)$$

This is the well-known value of T_K in the local moment regime (at half-filling), if one uses the standard notation $E_c \equiv U/2$ with $\mathcal{N} = 2$ (single channel). It clearly explains that one key step to the experimental observation of the Kondo effect in quantum dots[13] lies in the realization of strongly coupled structures, having Γ comparable to E_c in magnitude, such that the Kondo temperature remains accessible.

We finish by explaining precisely the restoration of full coherence below the Kondo temperature. In order to do this, we set the temperature to zero and perform an exact low-energy solution of the system of equations (25)–(30) (this was done in Appendix Ref. C of 40). This analysis, valid while $\delta E \neq 0$ for an arbitrary number of levels, leads to the following value of the zero-temperature, zero-frequency density of states in our approximation:

$$\rho_d(\omega = T = 0) = \frac{1}{\pi N_L \Gamma} \frac{\pi/2}{\mathcal{N}+1} \tan\left(\mathcal{N}\frac{\pi/2}{\mathcal{N}+1} \right). \qquad (36)$$

The interpretation of this relation is that, whenever the temperature is lower than T_K, the density of states is pinned at its noninteracting value, no matter how large the Coulomb energy E_c is. This reflects the presence of the Kondo resonance at low energy. The *exact* Friedel's sum rule, however, is $\rho_d^{\mathrm{exact}}(\omega = T = 0) = 1/(\pi N_L \Gamma)$, independently of $\mathcal{N}$. The difference between Eq. (36) and this exact result is a consequence of the decoupling approximation made above and is related to the non-Fermi-liquid features described in Ref. 40. This artifact is nevertheless quite small in practice, since Eq. (36) goes to the exact value for $\mathcal{N}$ large and is only 10% off for $\mathcal{N} = 2$. Friedel's sum rule provides also a simple explanation for the restoration of the unitary limit in the conductance below the Kondo temperature, since the Landauer formula (32) at zero temperature leads to

$$G(T = 0) = \frac{\mathcal{N}e^2}{h} [\pi N_L \Gamma \rho_d(0)]. \qquad (37)$$

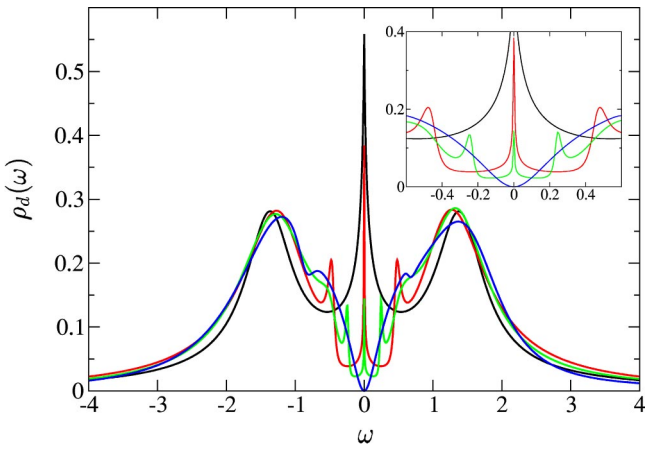

FIG. 1. Local density of states $\rho_d(\omega)$ at $E_c=1$, $\beta=800$, and fixed $W=(N_L-1)\delta E=1$ and $\Gamma^{\text{multi}}=N_L\Gamma=0.5$. The four curves correspond to different values of the number of levels in the dot: $N_L=1,3,5,\infty$ (from top to bottom, following the evolution of the central peak).

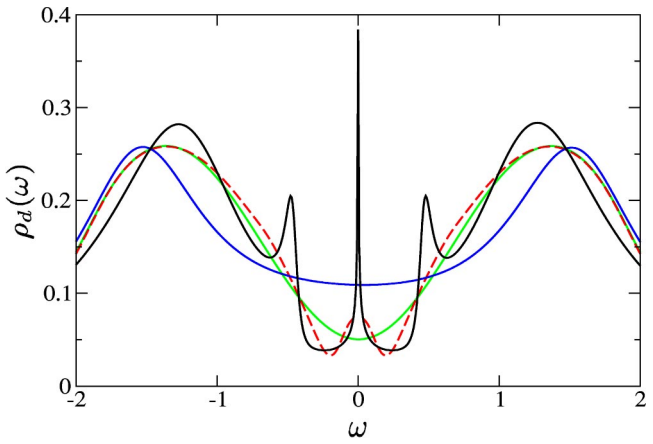

FIG. 2. Temperature dependence of $\rho_d(\omega)$ for the case $N_L=3$; temperatures correspond to $\beta=800$ (sharp central peak), $\beta=25$ (broad peak), $\beta=10$ (deep minima), and $\beta=2$ (shallow minima filled by thermal excitations).

3. Kondo effect: Numerical solution and crossover to the Coulomb blockade regime

The numerical solution of the set of self-consistent equations (25)–(30) allows us in principle to investigate all regimes of parameters. We will first concentrate on the gradual suppression of the Kondo effect with decreasing values of the single-level coupling Γ. In order to maintain the Coulomb blockade effect, we will keep in this section the total (multilevel) coupling fixed, $\Gamma^{\text{multi}}\equiv N_L\Gamma=0.5$, and vary the number of levels, N_L, to allow changes in $\Gamma=\Gamma^{\text{multi}}/N_L$. We will also fix the total bandwidth of the dot, $W=1$, so that the level spacing (assumed to be uniform) is also decreasing, $\delta E=W/(N_L-1)$. This way of proceeding allows us to interpolate from the few, well-separated levels, the situation relevant for small quantum dots in the Kondo regime, to the case of larger dots with small level spacing and many levels N_L, which shows only Coulomb blockade.

Figure 1 demonstrates indeed how the low-temperature local density of states evolves from $N_L=1$ (single level: regular Kondo effect) to $N_L=\infty$ (continuum of levels: Coulomb blockade only). In particular the rapid suppression of the Kondo peak for diminishing values of Γ at increasing N_L is in accordance with our previous discussion of the Kondo temperature, Eq. (35).

The temperature dependence of the electronic spectrum is presented for the three-level case $N_L=3$ in Fig. 2. When temperature is lowered, the zero-frequency density of states starts diminishing (by Coulomb blockade of states with different charge). One then reaches a minimum, before $\rho_d(0)$ begins shooting up, towards the unitarity limit (Friedel's sum rule) at zero temperature.

It is useful to compare this evolution of the density of states to the variations of the conductance $G(T,N_L)$ with temperatures, Fig. 3. This figure illustrates the reduction of the Kondo temperature with Γ by the downward shifting of the minimum of conductance. The Coulomb blockade is present at higher temperature, as shown by the decrease of $G(T)$ for $T_K<T<E_c^*$ upon lowering T.[16] For the last curve with a continuum of states in the dot, this behavior persists up to zero temperature. The inset in log scale on the same plot allows to grasp more clearly the saturation of conductance below the Kondo temperature.

C. Effects due to overlapping resonances in multilevel dots

The analysis in the previous section describes the usual situation where a crossover from the Coulomb blockade regime to the Kondo effect takes place as the temperature is lowered below the interlevel spacing in the dot. A different behavior can be expected when there is a set of overlapping resonances at low energies within the dot—i.e., an ensemble of levels of individual width greater than their separation, $\Gamma \gg \delta E$—which act together as a single effective level with enhanced coupling to the leads (the typical bandwidth of this set of level should also be smaller than the charging energy). The presence of broad resonances near the Fermi level can be relevant to some experimental situations.[35,36] Note that the

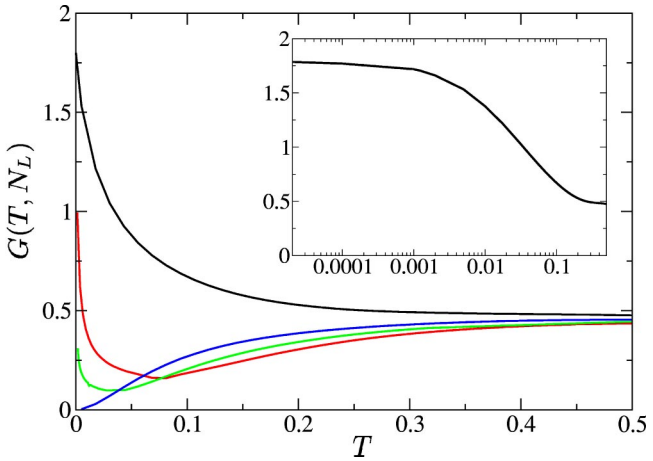

FIG. 3. Conductance $G(T,N_L)$ in units of e^2/h for the same parameters as in Fig. 1 as a function of temperature; curves with $N_L=1,3,5,\infty$ follow from top to bottom in the extreme left of the plot. Inset: $G(T,N_L=1)$ in temperature-logarithmic scale.

conductance distributions for open ballistic quantum dots, estimated from random matrix theory, are quite broad.[49,50] We give first some qualitative arguments in order to describe the new effects expected in this regime and then present explicit calculations using the integral equations.

1. Inverse crossover from the Kondo effect to Coulomb blockade

In practical situations encountered in quantum dots, the single-level Kondo temperature T_K is usually much smaller than the level spacing δE (which is typically comparable to E_c). Therefore Coulomb blockade occurs (if it does) inevitably before the Kondo effect sets in, as was shown at length in the previous section. There is, however, a simple mechanism that allows us to obtain Kondo temperatures *greater* than both level spacing and renormalized Coulomb energy E_c^*. The idea is that when the individual level width Γ exceeds the interlevel spacing δE, many levels are involved in the formation of the Kondo resonance. This leads to a ''multilevel Kondo temperature''[30,31]

$$T_K^{\text{multi}} \sim T_0 \exp\left(-\frac{\pi E_c}{2\mathcal{N} N_{eff} \Gamma} \right), \tag{38}$$

which can be greatly enhanced with respect to the single-level estimate, Eq. (35), by the presence of many levels $N_{eff} > 1$ acting together (increasing the number of channels $\mathcal{N}$ might also contributes to this effect). This way of enhancing the Kondo temperature allows us to obtain a new regime where $T_K^{\text{multi}} \gg E_c^*, \delta E$, so that the Kondo effect can now occur *before* the Coulomb blockade (when lowering the temperature), in an *inverse* manner as observed traditionally in quantum dots. The fact that the Coulomb energy can be strongly renormalized to smaller values adds credibility to this idea. One further notes that, at even lower temperatures, a Kondo peak associated with the formation of a resonance which involves only one electronic state in the dot will ultimately emerge. One therefore has a ''two-stage Kondo effect'' (if the single-level Kondo temperature is not vanishingly small).

In order to be more precise, we will first give a concrete example with a limiting case that one can understand independently of any approximation scheme. Then, we will illustrate in detail this ''inverse crossover'' using our integral equations.

2. Limit of exactly degenerate levels

We consider here the extreme limit in which N_L levels in the dot are simultaneously put to zero: $\epsilon_p = 0$ for all p (the total bandwidth W is therefore also zero). We can formulate the model after a redefinition of the fermionic operators (unitary transformation) $\{d_{p\sigma}^\dagger\} \to \{c_{p\sigma}^\dagger\}$, such that

$$c_{1\sigma}^\dagger = \frac{1}{\sqrt{N_L}} \sum_{p=1}^{N_L} d_{p\sigma}^\dagger . \tag{39}$$

In this case, the remaining fermionic degrees of freedom, $c_{p\sigma}^\dagger$ for $p > 1$, simply decouple from the problem, leaving an *effective single-level* Anderson model describing the fermion $c_{1\sigma}^\dagger$. Actually, a capacitive coupling persists between this fermion and all the other ones, but this influence gets frozen at low temperature. As the conductance through the dot is obtained from the Green's function

$$G_d^{loc}(\tau) \equiv \frac{1}{N_L} \sum_{pp'} \langle d_{p\sigma}^\dagger(0) d_{p'\sigma}(\tau) \rangle = \langle c_{1\sigma}^\dagger(0) c_{1\sigma}(\tau) \rangle, \tag{40}$$

one gets a full Kondo effect and a complete restoration of unitary conductance at low temperature. Furthermore, the width of this effective level is simply $N_L \Gamma$, as one checks by inserting $c_{1\sigma}^\dagger$ in Eq. (4). This leads then to an enhanced Kondo temperature

$$T_K^{\text{deg.}} = T_0 \exp\left(-\frac{\pi E_c}{2\mathcal{N} N_L \Gamma} \right), \tag{41}$$

as discussed in the introductory part of this section (because $\delta E = 0$ in this limiting case, one has $N_{eff} = N_L$).

We can easily check that our self-consistent scheme preserves this interesting property of the model. Indeed, when all levels ϵ_p are exactly degenerate ($W = 0$), one gets from Eq. (27) the f-electron Green's function $G_f(i\omega) = [i\omega - \Sigma_f(i\omega)]^{-1}$. We obtain therefore the Kondo effect of a single effective level.[40]

The following section will allow us to make this discussion more meaningful by studying the more realistic case of a quantum dot in the regime $\Gamma \gtrsim \delta E$, corresponding to nearly degenerate levels.

3. Inverse crossover: Illustration

We now illustrate the inverse crossover discussed qualitatively in Sec. IV C 1 by solving our integral equations in the regime $\Gamma \gtrsim \delta E$, where multilevel effects play an important role. We will assume here that $\Gamma \ll E_c$ so that one can neglect the single-level Kondo effect at low temperature (see, however, the next section). For this computation, we have fixed $\Gamma = 0.04$ and taken $N_L = 9$ states in the dot, varying the interlevel spacing from $\delta E = 0$ (exactly degenerate level case considered in the previous paragraph) to $\delta E = 0.01 \lesssim \Gamma$ (possibility of multilevel effect) to $\delta E = 0.08 > \Gamma$ (absence of multilevel effect).

The low-temperature local density of states displayed in Fig. 4 shows the expected multilevel enhanced Kondo peak at $\delta E = 0$ corresponding to formula (41). Upon increasing the level spacing to $\delta E = 0.01$, Coulomb blockade sets in at a scale $E_c^* < T_K^{multi}$; however, coherence effects remain around T_K^{multi} (since we are in a regime with $\delta E < \Gamma$). This results in a surprising splitting of the Kondo resonance at low energy. The last curve is taken with $\delta E = 0.08 > \Gamma$, so that no multilevel Kondo effect is possible, and only Coulomb blockade is observed. Another interesting consequence of this phenomenon is that the temperature dependence of the conductance is *reversed* with respect to the usual signature of the Kondo effect in quantum dots—i.e., to Fig. 3. Indeed, upon lowering the temperature, one notices an initial increase of the conductance (due to the multilevel Kondo effect), *then* a sharp decrease of the conductance because of the Coulomb block-

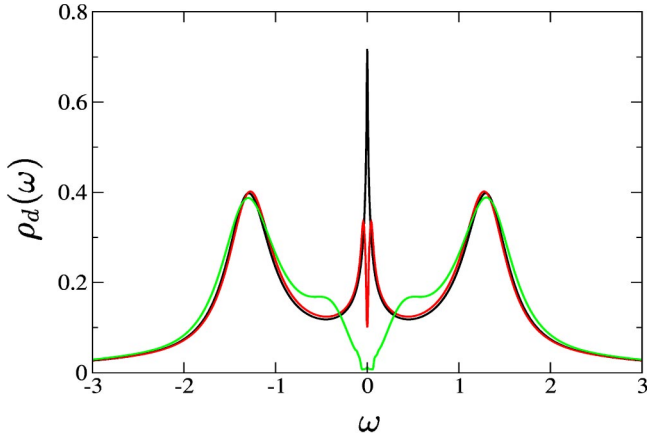

FIG. 4. Density of states $\rho_d(\omega)$ on the dot for $E_c=1$, $\Gamma=0.04$, inverse temperature $\beta=400$, $N_L=9$ states, and different values of the interlevel spacing: $\delta E=0,0.01,0.08$.

ade. This is illustrated by the middle curve in Fig. 5.

One can also perform a general evaluation of the multilevel Kondo temperature, starting from the leading behavior of the f Green's function at high temperature:

$$G_f^{loc}(i\omega)\simeq\frac{1}{N_L}\sum_p\frac{1}{i\omega-\epsilon_p}. \tag{42}$$

Equation (28) then leads to[58]

$$\alpha(i\nu)=-\frac{\mathcal{N}\Gamma}{\pi}\sum_p\ln\frac{\nu^2+|\epsilon_p|^2}{\nu^2+(|\epsilon_p|+T_0)^2}. \tag{43}$$

The Kondo temperature is reached when this kernel is of the order of E_c, so that one finds the final equation which determines $T_K^{\rm multi}$:

$$\prod_p\frac{(T_K^{\rm multi})^2+|\epsilon_p|^2}{(T_K^{\rm multi})^2+(|\epsilon_p|+T_0)^2}=\left(\frac{T_K}{T_0}\right)^2, \tag{44}$$

where T_K is the single-level Kondo temperature (35). A similar result was obtained previously by a renormalization

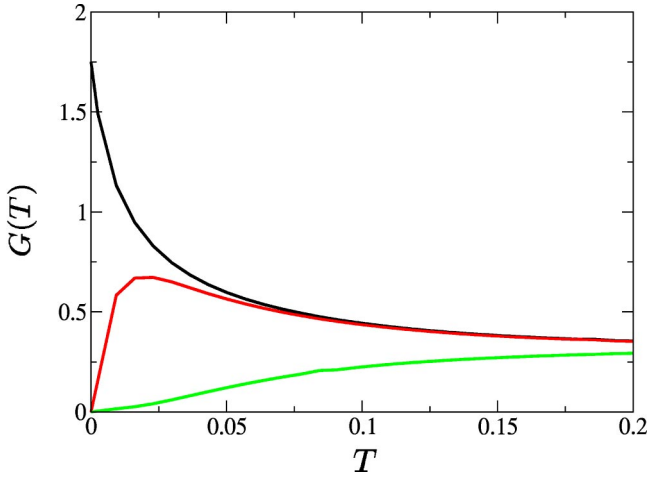

FIG. 5. Conductance $G(T)$ for the same parameters as in Fig. 4.

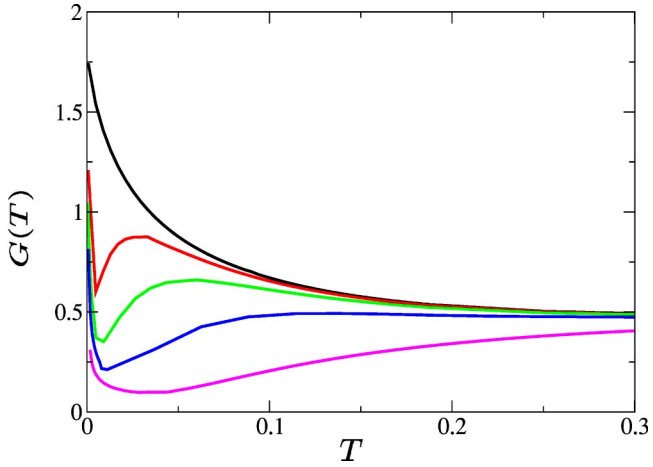

FIG. 6. Conductance $G(T)$ in the case $N_L=5$, $\Gamma=0.1$, and various level spacings: $\delta E=0,0.025,0.05,0.1,0.25$.

group argument.[30] The limiting cases studied before are obviously contained in the previous equation: $T_K^{\rm multi}$ reduces to T_K for widely separated levels (δE large) and in the opposite limit of exactly degenerate levels (or if $W\ll T_K^{\rm multi}$), $T_K^{\rm multi}=T_0(T_K/T_0)^{1/N_L}$, consistently with Eq. (41). In general, $T_K^{\rm multi}$ is enhanced with respect to the single-level Kondo temperature T_K. As an example, formula (44) shows that in the regime $\delta E\ll T_K^{\rm multi}\ll W\ll E_c$, one obtains then $T_K^{\rm multi}\sim T_0\exp[-\pi E_c\delta E/(2\mathcal{N}\Gamma T_K^{\rm multi})]$, so that the number of effective levels taking part to the multilevel Kondo resonance is $N_{eff}=T_K^{\rm multi}/\delta E$, as discussed qualitatively in Eq. (38).

We conclude this paragraph by summing up the physical picture that leads to the observed nonmonotonous conductance. In the case of many overlapping resonances, a quantum dot can be described as a small metallic grain dominated by Coulomb blockade at low temperature, which implies a vanishing zero-frequency density of states. Upon raising the temperature, many different charge states become available by the thermal smearing of the Coulomb blockade, and the conductance is rapidly increasing on a scale of the order of E_c^* (which is also the typical size of the dip observed in the split Kondo peak). Due to the large single-level width considered in this regime, all these energy levels can then act coherently as a localized spin degree of freedom that undergoes the Kondo effect. This explains the upturn of the conductance when temperature reaches the Kondo energy $T_K^{\rm multi}$.

4. Two-stage Kondo effect

Finally we consider again a multilevel case $\delta E\ll\Gamma$, but now with $\Gamma\lesssim E_c$, so that the single-level Kondo resonance is accessible to the low-temperature regime. Therefore, one witnesses a further increase of the conductance at low temperature, taking place after the inverse Kondo-to-Coulomb crossover that we discussed previously. The occurrence of such a "two-stage Kondo effect" is depicted for the conductances shown in Fig. 6. For this calculation, we have taken $N_L=5$ levels, $\Gamma=0.1$, and various level spacings between zero and 2.5Γ.

The two curves with $0<\delta E<\Gamma$ show indeed this two-stage Kondo effect: a first rise of the conductance at high

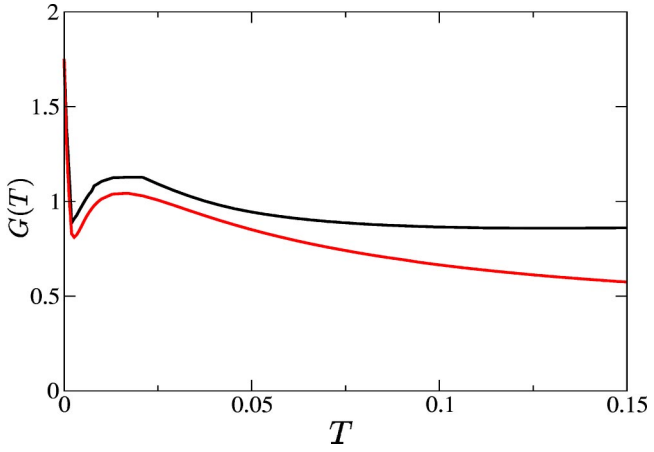

FIG. 7. Lower curve: conductance $G(T)$ in the case $N_L=5$, $\Gamma=0.1$, and $\delta E=0.015$. Upper curve: similar model, but ten additional levels (with larger spacing $\delta E'=0.2$) have been superimposed to the previous ones.

temperature due to the multilevel resonance at $T\sim T_K^{multi}$, then the Coulomb blockade at $T\sim E_c^*$, and then a further increase at $T\sim T_K$ (smallest scale of the problem). The last two curves, with $\delta E=0.1,0.25$, show the usual crossover that was illustrated in Fig. 3 in Sec. IV B 3.

A last point that was checked is that our results are weakly sensitive to the addition of more levels outside the energy window of width Γ. This calculation is shown in Fig. 7.

5. Summary of the different regimes of transport

A sketch of the different regimes analyzed in this paper is given in Fig. 8, as a function of the level spacing, δE, and single-level width, Γ. We assume that the number of electrons in the dot is odd, so that the ground state, in the absence of coupling to the leads, is degenerate. The transition between different regimes is a smooth crossover. We will not discuss in the following the effect of the renormalization of

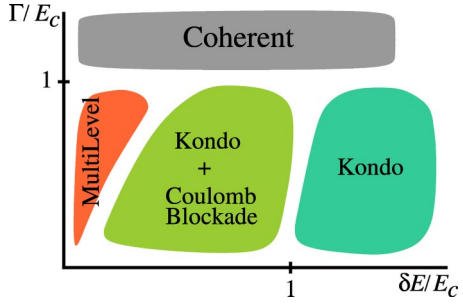

FIG. 8. Sketch of the different regimes discussed in the paper, as function of the charging energy, E_C, level spacing within the dot, δE, and level widths, Γ, with a constant number of levels. The notation "Kondo" corresponds to a single-level Kondo effect. The region "Kondo+Coulomb-Blockade" is the usual situation in quantum dots. The "Multilevel" region is also associated to the Kondo effect, but with important renormalization of the Kondo temperature, as discussed in the text. The "Coherent" regime stands for a temperature independent conductance.

the charging energy; therefore, the zone boundaries that locate the different regimes will not be determined here. However, this can be done in practice by solving the integral equations, as discussed in the main body of the paper. Also it would be interesting to perform a full renormalization group analysis of the renormalization of both T_K and E_c^* along the lines of Refs. 31 and 51.

The occurrence of Kondo effect is signaled by a nonmonotonous temperature dependence of the conductance and is observable at $\Gamma\ll\delta E$ for temperatures smaller than the single-level Kondo temperature T_K given by Eq. (35). Depending on the relative values of level spacing δE and Coulomb energy E_c, Coulomb blockade might also be present above the Kondo temperature, which is the usual experimental situation encountered in quantum dots. We emphasize that if Γ is much smaller than E_c, the Kondo temperature is extremely small and the Kondo effect inobservable in practice; this corresponds to weakly coupled dots, and this situation shows only Coulomb blockade. In the case $\delta E\ll\Gamma$ we have defined a region "multilevel" which corresponds actually to various regimes discussed previously. This describes the inverse crossover (Kondo to Coulomb blockade), as well as the two-stage Kondo effect shown in Sec. IV C 4. This region can also imply that the Kondo effect is observed in the usual manner, but with a Kondo temperature greater than the single-level estimate. Note that the Kondo effect involving many levels can also occur in dots with an even number of electrons, in a similar manner to the Kondo resonance which arises at a singlet-triplet crossing in an applied magnetic field.[52] Finally, the region $\Gamma\gg E_c$ of the diagram (denoted "Coherent") is associated with large conductances that are weakly modulated with temperature or applied gate voltage.

V. CONCLUSIONS

In this paper we have presented a method of calculation for strongly correlated mesoscopic systems in terms of a collective phase variable and the quasiparticle degrees of freedom. The scheme is valid both for the study of the Coulomb blockade regime and of the Kondo effect.

We have shown examples of the crossover between a Coulomb blockade regime at temperatures below the charging energy, and the formation of a Kondo resonance at temperatures lower than the separation between levels within the dot. In addition, we have described an inverse regime, where a Kondo-like resonance is split at low energies by Coulomb blockade effects. This regime is associated with the existence of many conduction channels or overlapping resonances within the dot, which contribute collectively to the Kondo effect. The coherence of this state is destroyed at low energies by Coulomb effects. At even lower energies, a narrow Kondo peak, associated with a single level within the dot, will emerge.

Because the self-consistent approach used here was successfully applied to a model of strongly correlated electrons (Hubbard model) in a previous work,[40] we can also envision possible applications of this work to the physics of granular materials or quantum dot arrays in the vicinity of the metal-insulator transition.[53–56] Disorder effects, which were ne-

glected here, should also be included in future work along these lines.

Other possible development is an exact (numerical) solution of the self-consistent action (11) and (12) instead of taking the spherical limit as was done in Sec. IV A, which brings some limitations (as the restriction to valleys of conduction). Also importantly, we believe that the present work, both by the technical concepts and the physical ideas, connects in an original manner the fields of strongly correlated systems and mesoscopic physics.

ACKNOWLEDGMENTS

S.F. and A.G. are grateful to D. Esteve, H. Pothier, and C. Urbina for a useful discussion. We appreciate the hospitality of the Kavli Institute of Theoretical Physics, where this work was initiated. The KITP is supported by the NSF through Grant No. PHY99-07949. P.S.J. and F.G. are thankful to MCyT (Spain) for financial support through Grant No. MAT2002-04095-C02-01. S.F. acknowledges the support of the CNRS-PICS(1062) program.

[1] M. Kastner, Rev. Mod. Phys. **64**, 849 (1992).
[2] *Single Electron Tunneling*, edited by H. Grabert and M. Devoret (Plenum Press, New York, 1992).
[3] Y. Alhassid, Rev. Mod. Phys. **72**, 895 (2000).
[4] I.L. Aleiner, P.W. Brouwer, and L.I. Glazman, Phys. Rep. **358**, 309 (2002).
[5] D.V. Averin and K.K. Likharev, in *Mesoscopic Phenomena in Solids*, edited by B.L. Altshuler, P.A. Lee, and R.A. Webb (Elsevier, New York, 1991).
[6] T.A. Fulton and G.J. Dolan, Phys. Rev. Lett. **59**, 109 (1987).
[7] P. Lafarge, H. Pothier, E.R. Williams, D. Esteve, C. Urbina, and M.H. Devoret, Z. Phys. B: Condens. Matter **85**, 327 (1991).
[8] P. Joyez, V. Bouchiat, D. Esteve, C. Urbina, and M.H. Devoret, Phys. Rev. Lett. **79**, 1349 (1997).
[9] J. Kondo, Prog. Theor. Phys. **32**, 37 (1964).
[10] A. Hewson, *The Kondo Problem to Heavy Fermions* (Cambridge University Press, Cambridge, England, 1996).
[11] L.I. Glazman and M.E. Raikh, JETP Lett. **47**, 452 (1988).
[12] T.K. Ng and P.A. Lee, Phys. Rev. Lett. **61**, 1768 (1988).
[13] D. Goldhaber-Gordon, H. Shtrikman, D. Mahalu, D. Abusch-Magder, U. Meirav, and M.A. Kastner, Nature (London) **391**, 156 (1998).
[14] S.M. Cronenwett, T.H. Oosterkamp, and L.P. Kouwenhoven, Science **281**, 540 (1998).
[15] L. Kouwenhoven and L. Glazman, Phys. World **14**, 33 (2001).
[16] L.I. Glazman and M. Pustilnik, in Proceedings of the NATO-ASI ''New Directions in Mesoscopic Physics,'' Erice, 2002, cond-mat/0302159.
[17] T.-L. Ho, Phys. Rev. Lett. **51**, 2060 (1983).
[18] E. Ben-Jacob, E. Mottola, and G. Schön, Phys. Rev. Lett. **51**, 2064 (1983).
[19] G. Göppert and H. Grabert, Phys. Rev. B **63**, 125307 (2001).
[20] F. Guinea and G. Schön, Europhys. Lett. **1**, 585 (1986).
[21] S.V. Panyukov and A.D. Zaikin, Phys. Rev. Lett. **67**, 3168 (1991).
[22] G. Schön and A.D. Zaikin, Phys. Rep. **198**, 237 (1990).
[23] G. Göppert, X. Wang, and H. Grabert, Phys. Rev. B **55**, 10 213 (1997).
[24] P. Joyez, D. Esteve, and M.H. Devoret, Phys. Rev. Lett. **80**, 1956 (1998).
[25] D.S. Golubev, J. König, H. Schoeller, G. Schön, and A.D. Zaikin, Phys. Rev. B **56**, 15 782 (1997).
[26] C.P. Herrero, G. Schön, and A.D. Zaikin, Phys. Rev. B **59**, 5728 (1999).
[27] P.W. Anderson, Phys. Rev. **124**, 41 (1961).
[28] Y. Meir, N.S. Wingreen, and P.A. Lee, Phys. Rev. Lett. **66**, 3048 (1991).
[29] M. Pustilnik and L.I. Glazman, Phys. Rev. Lett. **87**, 216601 (2001).
[30] K. Yamada, K. Yosida, and K. Hanzawa, Prog. Theor. Phys. **71**, 450 (1984).
[31] T. Inoshita, A. Shimizu, Y. Kuramoto, and H. Sakaki, Phys. Rev. B **48**, 14 725 (1993).
[32] T. Pohjola, J. König, M.M. Salomaa, J. Schmid, H. Schoeller, and G. Schön, Europhys. Lett. **40**, 189 (1997).
[33] J.J. Palacios, L. Liu, and D. Yoshioka, Phys. Rev. B **55**, 15 735 (1999).
[34] A.L. Yeyati, F. Flores, and A. Martín-Rodero, Phys. Rev. Lett. **83**, 600 (1999).
[35] P.G. Silvestrov and Y. Imry, Phys. Rev. Lett. **85**, 2565 (2000).
[36] P.G. Silvestrov and Y. Imry, Phys. Rev. B **65**, 035309 (2001).
[37] W. Hofstetter and H. Schoeller, Phys. Rev. Lett. **88**, 016803 (2002).
[38] F. Guinea, Phys. Rev. B **67**, 195104 (2003).
[39] C. Fühner, U.F. Keyser, R.J. Haug, D. Reuter, and A.D. Wieck, Phys. Rev. B **66**, 161305 (2002).
[40] S. Florens and A. Georges, Phys. Rev. B **66**, 165111 (2002).
[41] T. Pruschke and N. Grewe, Z. Phys. B: Condens. Matter **74**, 439 (1989).
[42] O. Parcollet and A. Georges, Phys. Rev. Lett. **79**, 4665 (1997).
[43] D. Chouvaev, L.S. Kuzmin, D.S. Golubev, and A.D. Zaikin, Phys. Rev. B **59**, 10 599 (1999).
[44] N.E. Bickers, Rev. Mod. Phys. **59**, 845 (1987).
[45] S. Renn cond-mat/9708194 (unpublished).
[46] S. Drewes, D.P. Arovas, and S. Renn cond-mat/0301396 (unpublished).
[47] S. Sachdev, *Quantum Phase Transitions* (Cambridge University Press, Cambridge, England, 2000).
[48] T.A. Costi, in Proceedings of the 2nd Hvar Workshop ''Concepts in Correlated Electrons,'' cond-mat/0212651.
[49] H.U. Baranger and P.A. Mello, Phys. Rev. Lett. **73**, 142 (1994).
[50] R.A. Jalabert, J.-L. Pichard, and C.W.J. Beenakker, Europhys. Lett. **27**, 255 (1994).
[51] J. König and H. Schoeller, Phys. Rev. Lett. **81**, 3511 (1998).
[52] D. Giuliano, B. Jouault, and A. Tagliacozzo, Phys. Rev. B **63**, 125318 (2001).

[53] D.P. Arovas, F. Guinea, C. Herrero, and P. San José, Phys. Rev. B **68**, 085306 (2003). .
[54] K.B. Efetov and A. Tschersich, Europhys. Lett. **59**, 114 (2002).
[55] C.A. Stafford and S. DasSarma, Phys. Rev. Lett. **72**, 3590 (1994).
[56] A.V. Herzog, P. Xiong, F. Sharifi, and R.C. Dynes, Phys. Rev. Lett. **76**, 668 (1996).
[57] We have renormalized the Coulomb energy by a factor of 2 to obtain the correct solution in the atomic limit; see Ref. 40.
[58] Naively the cutoff T_0 in this expression should be of order Λ as implied by the regularized expression of the bath, $\Delta(\tau) = -N_L\Gamma[1-\exp(-\Lambda|\tau|)]/(\pi\tau)$. However, logarithmic corrections to our approximative derivation imply that $T_0 \sim \sqrt{E_c\Gamma}$.